AIAA 96-4562

Navigation and Guidance for the Mars Surveyor '98 Mission

Pieter H. Kallemeyn, Jr., Philip C. Knocke, P. Daniel Burkhart and Sam W. Thurman

Jet Propulsion Laboratory
California Institute of Technology
Pasadena, CA

AIAA/AAS Astrodynamic Specialist Conference
August 10-12, 1998 / Boston, MA

NAVIGATION AND GUIDANCE FOR THE MARS SURVEYOR '98 MISSION

Pieter H. Kallemeyn, Jr.*, Philip C. Knocke†,
P. Daniel Burkhart‡, Sam W. Thurman§

Jet Propulsion Laboratory
California Institute of Technology
Pasadena, California

Abstract

In December, 1998 and January 1999 NASA will launch an orbiter and lander to Mars as part of the overall Mars Exploration Program managed at JPL. The two missions pose interesting navigation challenges during the interplanetary cruise phase. The orbiter needs to be delivered to Mars with an error in its capture orbit's periapsis no greater than 20 km, while the lander's delivery requirements is a flight path angle error upon atmosphere entry no larger that 0.25°. Navigation and guidance analysis performed at the Jet Propulsion Laboratory in support of mission planning has shown that the expected guidance error meets mission requirements for the lander. Monte-Carlo simulation of the interplanetary cruise phase provide statistical data of required ΔV for each midcourse maneuver. These results have determined the quantity of propellant needed to obtain a 95% probability of successfully completing the interplanetary cruise phase for both spacecraft.

Mission and Flight Systems Overview

Mars Surveyor 98 is part of NASA's Mars Surveyor Program, a scientifically aggressive but tightly cost-constrained program of robotic Mars exploration, with the goal of sending two spacecraft to Mars every two years from 1997 to 2006 [1]. During the 1998 opportunity, the Mars Climate Orbiter and Mars Polar Lander, both built under a system contract with Lockheed Martin Astronautics (LMA), will be launched aboard Boeing Delta II 7425 launch vehicles. These missions comprise the Mars Surveyor 1998 Project, managed by the Jet Propulsion Laboratory for NASA.

Launching in December 1998, the Mars Climate Orbiter is destined for a two-year study of the martian atmosphere and surface, from the vantage of a low circular orbit around Mars. It carries a rebuilt version of the Pressure Modulator Infrared Radiometer (PMIRR), an atmospheric sounding instrument (the original PMIRR was lost aboard the Mars Observer spacecraft in August 1993), and the Mars Color Imager (MARCI). Figure 1 illustrates the spacecraft configuration on orbit. The orbiter is solar powered, and uses reaction wheels for attitude control during most of the mission. A suite of eight monopropellant thrusters is used for reaction wheel momentum management and for all translational maneuvers, except for Mars orbit insertion, which utilizes the bipropellant main engine.

Four trajectory correction maneuvers (TCM's) are planned during the nine month cruise phase to correct launch vehicle injection errors and to establish the proper arrival conditions. The bipropellant main engine is used only once, to propulsively insert the spacecraft into a 14-21 hour capture orbit in late September to early October, 1999. After a trim maneuver to reduce the orbit period further, the spacecraft starts the first of more

---

* Senior Staff Engineer, Navigation and Flight Mechanics Section
† Senior Staff Engineer, Mission and Systems Architecture Section
‡ Staff Engineer, Navigation and Flight Mechanics Section
§ Mars Surveyor '98 Project Engineer

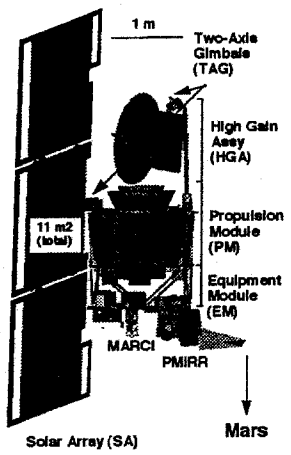

Figure 1 - Mars Climate Orbiter

than 200 passes through the upper atmosphere of Mars, to gradually circularize the orbit. This aerobraking phase is designed to be completed at least two weeks prior to arrival of the Mars Polar Lander in early December, 1999. Once aerobraking is completed, the monopropellant thrusters are used to insert the spacecraft into a near-circular, near-polar orbit at an altitude of 405 km. From December to March, 2000, the orbiter serves as a command and data relay asset for the Mars Polar Lander. The interval from March 2000 to January 2002 is the primary science phase for the orbiter. Afterward, the orbiter may be used as a data relay asset for future landers. Figure 2 summarizes the major mission phases, key events, and configuration changes during the orbiter's mission.

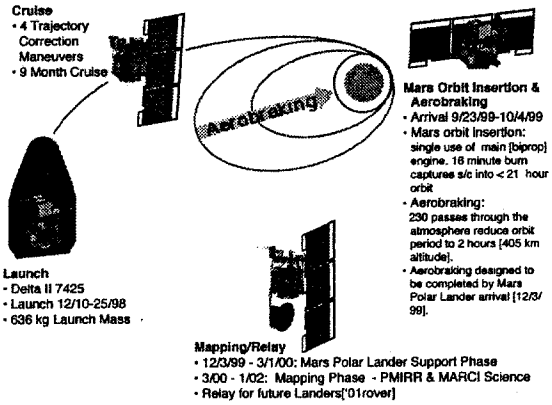

Figure 2 - Mars Climate Orbiter Mission

The objective of the Mars Polar Lander mission is a soft landing on the south polar layered terrain of Mars, followed by a three month science mission. The science payload includes an integrated suite of geochemistry and meteorology instruments called the Mars Volatiles and Climate Surveyor (MVACS), as well as the Mars Descent Imager (MARDI), and a Lidar instrument supplied by the Russian Institute for Space Science. Figure 3 shows an expanded view of the lander, its protective aeroshell, and the cruise stage.

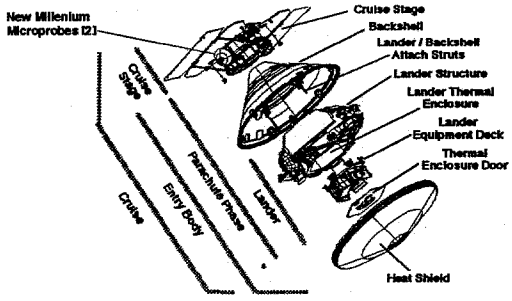

Figure 3 - Mars Polar Lander Flight System

The majority of spacecraft functions are performed by the lander, contained during cruise and entry within the aeroshell. Midcourse corrections and three-axis attitude control during cruise and hypersonic entry are performed using a suite of eight monopropellant thrusters, scarfed through openings in the backshell (the aft portion of aeroshell). The cruise stage, which is jettisoned five minutes before entry, is comprised of a composite ring structure to which are attached four solar panels, redundant star cameras and sun sensors, and low- and medium-gain radio antennas. In addition, two experimental microprobes are carried to Mars attached to the cruise stage; these probes deploy themselves automatically approximately ten seconds after the cruise stage is jettisoned by the lander.

Following hypersonic entry, the heatshield is jettisoned, a parachute is deployed. Finally, the lander is released from the backshell. The lander then performs a powered descent to a soft landing using radar-aided inertial guidance. Figure 4 summarizes the mission phases and key events during the lander's mission.

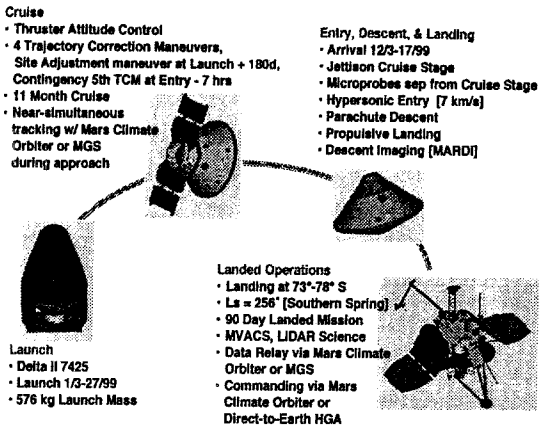

Figure 4 - Mars Polar Lander Mission

Mission Design

The interrelationships between the orbiter and lander missions required an integrated approach to the Mars Surveyor '98 mission design, balancing risk and science return across both missions, while staying within launch vehicle and spacecraft constraints. Both spacecraft use a type II transfer trajectory (greater than 180° transfer angle).

Figure 5 summarizes launch and arrival conditions for the Orbiter during its launch period from December 10 - December 25, 1998.

Day in Launch Period		1	2	3	4	5	6	7	8
Phase		Primary	Primary	Primary	Primary	Primary	Primary	Primary	Primary
Launch Date		12/10/98	12/11/98	12/12/98	12/13/98	12/14/98	12/15/98	12/16/98	12/17/98
Arrival Date		9/23/99	9/23/99	9/23/99	9/23/99	9/23/99	9/23/99	9/23/99	9/23/99
Launch Energy	[km2/s2]	11.03	10.89	10.75	10.64	10.55	10.48	10.43	10.40
Approach Velocity	[km/s]	3.34	3.34	3.35	3.35	3.35	3.36	3.37	3.37
Descending Node Solar Time	[deg.]	6:16PM	6:18PM	6:20PM	6:21PM	6:23PM	6:25PM	6:27PM	6:29PM

Day in Launch Period		9	10	11	12	13	14	15	16
Phase		Secondary	Secondary	Secondary	Secondary	Secondary	Secondary	Contingency	Contingency
Launch Date		12/18/98	12/19/98	12/20/98	12/21/98	12/22/98	12/23/98	12/24/98	12/25/98
Arrival Date		9/24/99	9/24/99	9/24/99	9/24/99	9/26/99	9/29/99	10/1/99	10/4/99
Launch Energy	[km2/s2]	10.41	10.44	10.51	10.61	10.44	10.28	10.14	10.01
Approach Velocity	[km/s]	3.38	3.39	3.41	3.42	3.42	3.42	3.43	3.44
Descending Node Solar Time [PM]	[deg.]	6:31PM	6:34PM	6:36PM	6:39PM	6:29PM	6:19PM	6:10PM	6:00PM

Figure 5 - Orbiter Launch/Arrival Dates

The orbiter launch/arrival dates have been chosen to stay within launch vehicle constraints defined by maximum launch energy (C3 ≈ 11 km^2/s^2) and maximum declination of the launch asymptote (28.5°) for the given launch mass, while maximizing the probability of the orbiter completing aerobraking before lander arrival. The result is a nearly constant arrival date during the first 12 days of the orbiter launch period, followed by a slip in arrival dates to prevent high launch declinations. The first eight days are designated the "Primary" launch period. During this time the launch probability is expected to be in excess of 98%. It is required that the orbiter have a 95% or greater probability of completing aerobraking if launched within its Primary launch period. A six day Secondary and a two day Contingency launch period follow. In order to improve launch probability, two launch opportunities per day are used during the orbiter launch period.

Lander mission constraints include maximum allowable launch energy [$C_3 \approx 11$ km^2/s^2], and a requirement to avoid landing on CO_2 frost at the desired arrival latitudes and season. In addition, it is required that at least nine days separate the end of the orbiter launch period (December 25, 1998) and the start of the lander launch period, assuming the availability of both Delta launch pads. This places the earliest launch date on January 3, 1999, and the earliest arrival date on December 3, 1999. Another constraint is the maximum entry velocity (7.07 km/s) allowed for the heatshield design. Finally, in order to land on the polar layered terrain, the lander must get as far south as possible. Figure 6 illustrates the relationship between launch/arrival dates, entry velocity, and maximum accessible southern latitude.

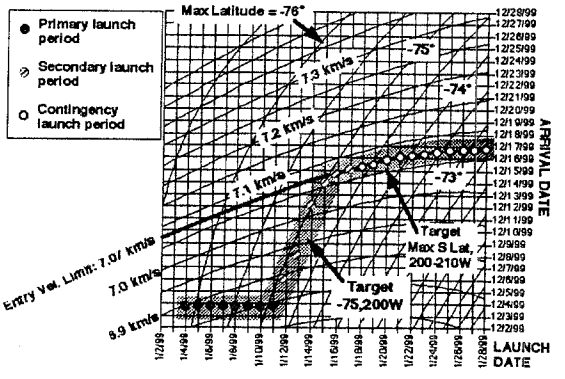

Figure 6 - Lander Launch/Arrival Strategy

Like the orbiter, the lander's launch period is broken into an eight day Primary, and a six day Secondary launch period. The Primary interval is characterized by a constant arrival date (December 3, 1999). The launch/arrival strategy for the Secondary period allows the arrival date to slip, and entry velocity to increase, in order to maintain access to sites as far south as -75°. During the Contingency launch period, a launch/arrival strategy is followed which targets the lander to the maximum southern latitude consistent with the entry velocity limit. The total duration of the lander launch period is 25 days. A single launch opportunity per day is used during this time. Figure 7 summarizes launch and arrival conditions during the launch period.

Day in Launch Period	1	2	3	4	5	6	7	8
Phase	Primary	Primary	Primary	Primary	Primary	Primary	Primary	Primary
Launch Date	1/3/99	1/4/99	1/5/99	1/6/99	1/7/99	1/8/99	1/9/99	1/10/99
Arrival Date	12/3/99	12/3/99	12/3/99	12/3/99	12/3/99	12/3/99	12/3/99	12/3/99
Launch Energy [km2/s2]	11.15	10.90	10.65	10.42	10.20	9.98	9.78	9.57
Entry Velocity [km/s]	6.91	6.90	6.89	6.88	6.87	6.86	6.85	6.85
Landing Latitude [deg.]	-75.0	-75.0	-75.0	-75.0	-75.0	-75.0	-75.0	-75.0

Day in Launch Period	9	10	11	12	13	14
Phase	Secondary	Secondary	Secondary	Secondary	Secondary	Secondary
Launch Date	1/11/99	1/12/99	1/13/99	1/14/99	1/15/99	1/16/99
Arrival Date	12/5/99	12/7/99	12/12/99	12/14/99	12/14/99	12/15/99
Launch Energy [km2/s2]	9.55	9.56	9.79	9.82	9.61	9.53
Entry Velocity [km/s]	6.89	6.93	7.02	7.07	7.06	7.07
Landing Latitude [deg.]	-75.0	-75.0	-75.0	-75.0	-75.0	-75.0

Day in Launch Period	15	16	17	18	19	20	21	22
Phase	Contingency	Contingency	Contingency	Contingency	Contingency	Contingency	Contingency	Contingency
Launch Date	1/17/99	1/18/99	1/19/99	1/20/99	1/21/99	1/22/99	1/23/99	1/24/99
Arrival Date	12/15/99	12/15/99	12/15/99	12/15/99	12/16/99	12/16/99	12/16/99	12/16/99
Launch Energy [km2/s2]	9.35	9.18	9.03	8.91	8.86	8.76	8.68	8.62
Entry Velocity [km/s]	7.07	7.06	7.06	7.05	7.07	7.06	7.06	7.06
Landing Latitude [deg.]	-74.8	-74.6	-74.5	-74.3	-74.2	-74.0	-73.8	-73.5

Day in Launch Period	23	24	25
Phase	Contingency	Contingency	Contingency
Launch Date	1/25/99	1/26/99	1/27/99
Arrival Date	12/16/99	12/16/99	12/17/99
Launch Energy [km2/s2]	8.57	8.53	8.53
Entry Velocity [km/s]	7.06	7.05	7.07
Landing Latitude [deg.]	-73.3	-73.1	-73.0

Figure 7 - Lander Launch/Arrival Data

Navigation and Guidance Requirements

For the Mars Surveyor '98 missions, the most stringent requirements apply to the lander. A relatively shallow entry flight path angle of -13.25° was chosen, to maximize both downrange travel (and hence the southern-most latitude) and site elevation access-ibility. Earth-based radar indicates that the targeted landing sector covering latitudes 73°-78° south and longitudes 170°-230° west has landing site elevations as high as 5 km. Also, in order to prevent large landing dispersions, which would adversely affect science return and increase the landed environmental envelope, entry angle control is required to be no greater than ±0.25° (95% probability). The orbiter is required to be targeted such that the variation in capture orbit periapse altitude is no greater than ±20 km (99% probability) [2].

Navigation Strategy

The navigation strategy for both the orbiter and lander is based on that devised for the Mars Pathfinder mission [3]. In general, this involves collecting radio metric tracking data at regular intervals for flight path estimation, predicting the arrival conditions, and performing occasional midcourse maneuvers, when needed, to correct the flight path such that the required arrival conditions are achieved.

Tracking Data

Both vehicles will be tracked at regular intervals from ground stations of the Deep Space Network (DSN) located in California, Australia, and Spain. The DSN's 34-m antenna subnet will be used to perform two-way Doppler tracking and ranging, in conjunction with command and telemetry operations, at X-band frequencies (7.2-8.4 Ghz) during cruise. The Doppler data provide measurements of the average range-rate from the spacecraft to the station, and are accurate to 0.05 mm/s (1σ) or better over 60 second averaging intervals. The ranging system measures the round-trip time delay from the station to the spacecraft and back, and, when properly calibrated for station and spacecraft electronic delays, is accurate to 1 m (1σ) or better. These measurement errors are consistent with those observed during the Mars Pathfinder and Mars Global Surveyor missions [3,4]. Table 1 shows the tracking coverage assumed for navigation error analysis. In addition, measurements of the ionosphere and water vapor are made at the DSN sites and processed into calibrations to be applied to the tracking data.

Table 1: Tracking coverage schedule

Mission Phase	Time Period	Tracking frequency
Launch	L+0 d to L+30 d	1 pass per day
Cruise	L+30 d to M-45 d	3 passes per week
TCM coverage	TCM-3 d to TCM+3 d	1 pass per day
Approach	M-45 d to M-0 d	3 passes per day

Orbit Determination

The flight path estimation, or orbit determination, process involves estimating the spacecraft's flight path and a set of force model and measurement error model parameters from the tracking data. This is accomplished with JPL's multi-mission navigation software system, which employs a discrete sequential filtering algorithm for data reduction. The achievable accuracy depends upon data quantity and quality, observation geometry, and ultimately, the fidelity of the underlying models.

Parameters affecting the flight path include the initial state vector, solar radiation pressure model, planetary ephemeris and gravity modelling, and spacecraft-induced forces such as maneuvers and thruster-controlled attitude maintenance. The orbiter uses momentum wheels to control its attitude during cruise. Although infrequent, thruster events performed for momentum management impart small velocity changes to the spacecraft, which produce measurable effects on the flight path given sufficient time. These perturbations must be modeled carefully in the estimation process, in order to achieve acceptable navigational accuracy. These momentum unloading events are expected to occur approximately once every seven days during cruise.

Lander Small Forces Modelling

The lander does not have momentum wheels, but instead relies on thrusters alone to control its attitude within predetermined deadbands about the Earth direction (to maintain communication capability) and the Sun direction (to maintain solar array output). The short pulse width thruster firings used for attitude control have a random component that is difficult to reconstruct (and predict) accurately. Therefore, the spacecraft is programmed to monitor each thruster event, recording information on the attitude of the spacecraft at that time, what thrusters were activated, and the commanded pulse width for each thruster. This data is relayed down in telemetry and combined with a model of the propulsion system to produce a 'small forces file', which is a history of the velocity change produced by every thruster firing throughout cruise. This is the first time an interplanetary mission has attempted to record and model individual impulses on this scale. From results of ground testing of the thrusters, it is expected this model will be 80% accurate. The remaining error will be accounted for in the orbit determination process via a stochastic acceleration model.

Table 2 gives a summary of the principal orbit determination error sources and their associated modeling assumptions. Error sources such as atmospheric media, terrestrial polar motion, and the lander's attitude control mismodelling, are assumed to be random in nature, and are modeled as first-order Gauss-Markov processes. For these error sources, Table 2 also gives the assumed steady-state uncertainty and correlation time. Parameters listed in Table 2 without these values, such as solar pressure parameters, station locations, initial position and velocity, were assumed to be random biases.

Near-Simultaneous Tracking

The final 45 days of flight is the most critical for lander navigation, therefore tracking coverage is increased from 1 to 3 passes per day. Starting 30 days before lander arrival, tracking data from the lander will be combined with tracking data from either the orbiter (which would be aerobraking during this time) or the Mars Global Surveyor. This technique of combining tracking data from two spacecraft has been dubbed "near-simultaneous tracking". By combining tracking data and estimating the trajectories

Table 2: Orbit Determination Error Sources

Doppler noise (1σ): 0.05 mm/sec (60-s count time)
Range noise (1σ): 0.6 m (lander), 1.0 m (orbiter)

Filter Parameter	*a priori* uncertainty (1σ)	Process Noise (N/A for bias parameters)	Correlation time (N/A for bias parameters)	Comments
Initial position and velocity	100 km and 1.0 km/s	N/A	N/A	
Solar Pressure	50-100% for reflectivity, 1% for area	N/A	N/A	
Lander attitude control activity	0.27E-6 mm/ s^2 to 0.86E-6 mm/s^2	0.27E-6 mm/ s^2 to 0.86E-6 mm/s^2	0.0 hour	Stochastic
Orbiter momentum wheel desaturation			N/A	every seven days
TCM magnitude	0.66%	N/A	N/A	
Station Range Bias	0.6 m	0.6 m	0.0 days	Stochastic
S/C Range Bias	1 m	N/A	N/A	
Troposphere	4 cm	4 cm	3 hours	Stochastic
Ionosphere	3 cm (day) 1 cm (night)	3 cm (day) 1 cm (night)	5 hours (day) 24 hours (night)	Stochastic
Station locations	5 cm	N/A	N/A	
Polar motion	5 cm	5 cm	48 hours	Stochastic
Earth rotation	0.3 ms	0.3 ms	24 hours	Stochastic
Mars ephemeris	0.5 km (radial) 3.0 km (transverse) 6.0 km (normal)	N/A	N/A	

of both spacecraft simultaneously, the effects of error sources that are common to both spacecraft are dramatically reduced, due to their high degree of correlation. These common error sources include DSN station locations, Earth orientation, troposphere and ionosphere delay, Earth and Mars ephemeris. The result is a more accurate estimate of the lander's trajectory with respect to Mars than can be obtained via reduction of the lander tracking data set only.

Midcourse Guidance

At planned intervals, midcourse corrections, or trajectory correction maneuvers (TCM's), are computed and implemented to null guidance errors identified by navigation. Course corrections are computed using a high precision trajectory integration and search program, called SEPV [5]. This program is used widely for interplanetary missions conducted by JPL. SEPV is designed to solve the two-point boundary value problem which establishes the required maneuver parameters to null the difference between the predicted versus desired arrival conditions.

At a specified maneuver epoch, SEPV performs a high-precision, Gauss-Newton (or non-linear algorithm, if desired) search to find the velocity change vector, and subsequently the associated propulsive bum direction, start time, and duration needed to achieve a target set of arrival conditions. Each spacecraft implements a maneuver by slewing to align its net thrust vector with the desired velocity change, initiating the bum at the commanded start time, then commanding cut-off via closed-loop control once the target value of velocity change has been achieved.

Guidance Error Analysis Results

Two program sets were used to determine the expected guidance error for each spacecraft. JPL's Double-Precision Trajectory (DPTRAJ) Program Set and the Orbit Determination Program (ODP) Set, which are both used operationally as well as for pre-flight analysis [6,7]. Another software set used was JPL's Maneuver Operations Program Set (MOPS), in particular the programs INJCOV (Injection Covariance mapping) and LAMBIC (Linear Analysis of Maneuvers with Bounds and Inequality Constraints). LAMBIC is used to compute guidance error and ΔV statistics via Monte-Carlo simulation, using matrices generated by INJCOV and ODP.

For evaluation against the mission requirements, these guidance error covariances were mapped to the Mars-centered, Mars-Mean-Equator of Date B-plane (Fig. 8). The B-plane is a convenient coordinate frame for expressing guidance and navigation results for interplanetary missions. The B-plane is perpendicular to the incoming asymptote (known as the S-direction) and contains the two axes **R** and **T**. **T** is defined as the intersection of the B-plane with the Mars mean equator of date. The guidance uncertainty is expressed by a two-dimensional dispersion ellipse in the B-plane with semi-major axis, semi-minor axis, and orientation angle θ, and by the uncertainty in the time of arrival.

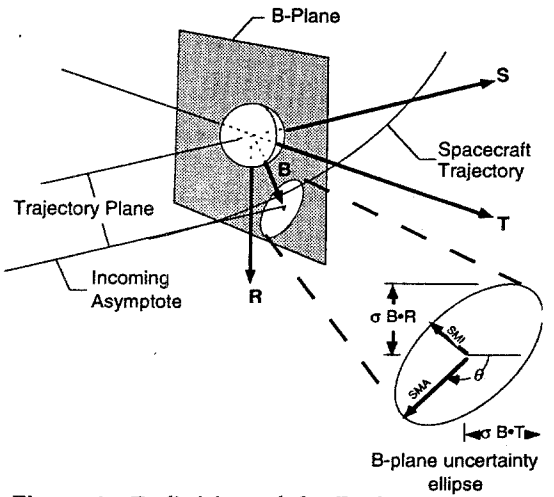

Figure 8: Definition of the B-plane coordinate frame

The ±20 km periapsis error (99% probability) requirement for the orbiter is compared to the orbiter's 3σ uncertainty ellipse, while the lander's ±0.25 flight path angle error (95% probability) for the lander is compared to the lander's 2σ ellipse. Lines on the B-plane were drawn that correspond to the acceptable limits of periapsis distance (for the orbiter) or flight path angle (for the lander). Figures 9 and 10 show the B-plane guidance uncertainty for the orbiter and lander, respectively. The area in-between the two lines on each B-plane figure indicate the region where the mission requirements are satisfied. The guidance error ellipses should lie entirely within these two lines. Tables 3 and 4 show numerical results after injection and every maneuver for the orbiter (3σ) and lander (2σ), respectively.

In Figure 10, the lander's 2σ guidance error after TCM-4 is slightly larger than the 0.25° flight path angle error requirement. This indicates that, although there is a high (>90%) probability of a <0.25° error in flight path angle after TCM-4, TCM-5 is still required as a contingency in order to provide the 95% probability confidence required by the mission. Figure 9 shows that the orbiter's 3σ guidance error after the fourth TCM is about 75% larger that the B-magnitude limits. This result implies a 91% probability of meeting the ±20 km periapsis radius error, not the 99% probability required by the mission. This is not a great concern for two reasons. First, the orbiter guidance analysis used a conservative error model for momentum desaturation, which contributes significantly to the overall guidance uncertainty. Additionally, these results do not assume that near-simultaneous tracking is used for the orbiter's approach. The project is planning to use this technique for the orbiter (using MGS as the orbiting reference spacecraft) as a means to further rehearse the navigation-related procedures required for the lander's approach.

Table 3: Orbiter guidance uncertainty
(Mars Mean Equator of Date B-plane)

	Relative Date	3σ B-plane ellipse			3σ time of flight uncertainty (seconds)	3σ periapsis uncertainty. (km)
		Semi-Major axis (km)	Semi-Minor axis (km)	Orientation angle, [θ] (deg)		
Injection	Launch+0 days	1,635,000	166,800	49.7	1,472,256	N/A
TCM-1	Launch+15 days	73,950	8,151	43.1	51,420	N/A
TCM-2	Launch+45 days	5,493	698.1	35.7	2,992	N/A
TCM-3	Arrival-60 days	385.8	324.6	13.8	47.5	276.0
TCM-4	Arrival-10 days	41.46	20.88	-72.0	6.50	35.3

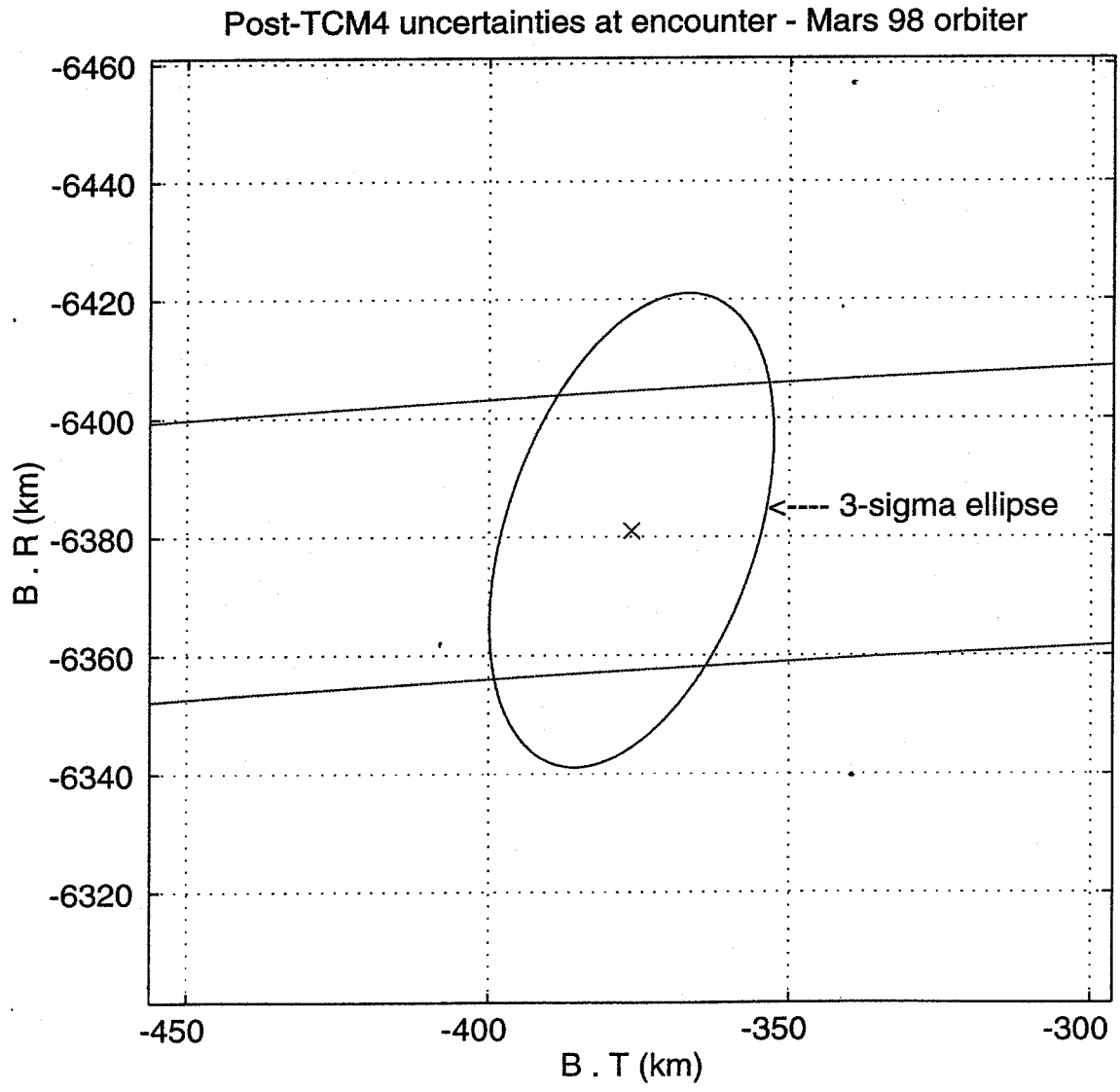

Table 4: Lander guidance uncertainty
(Mars Mean Equator of Date B-plane)

	Relative Date	2σ B-plane ellipse			2σ time of flight uncertainty (seconds)	2σ entry flight path uncertainty. [γ] (deg)
		Semi-Major axis (km)	Semi-Minor axis (km)	Orientation angle, [θ] (deg)		
Injection	Launch+0 days	3,470,000	101,100	17.6	275,616	N/A
TCM-1	Launch+15 days	38,800	1,391	18.6	3,396	N/A
TCM-2	Launch+45 days	2,596	58.82	17.8	171.5	N/A
TCM-3	Arrival-60 days	57.48	39.02	85.1	9.178	N/A
TCM-4	Arrival-4 days	6.052	2.262	-75.1	0.408	0.27
TCM-5	Arrival-7 hours	4.850	0.246	-76.7	0.138	0.24

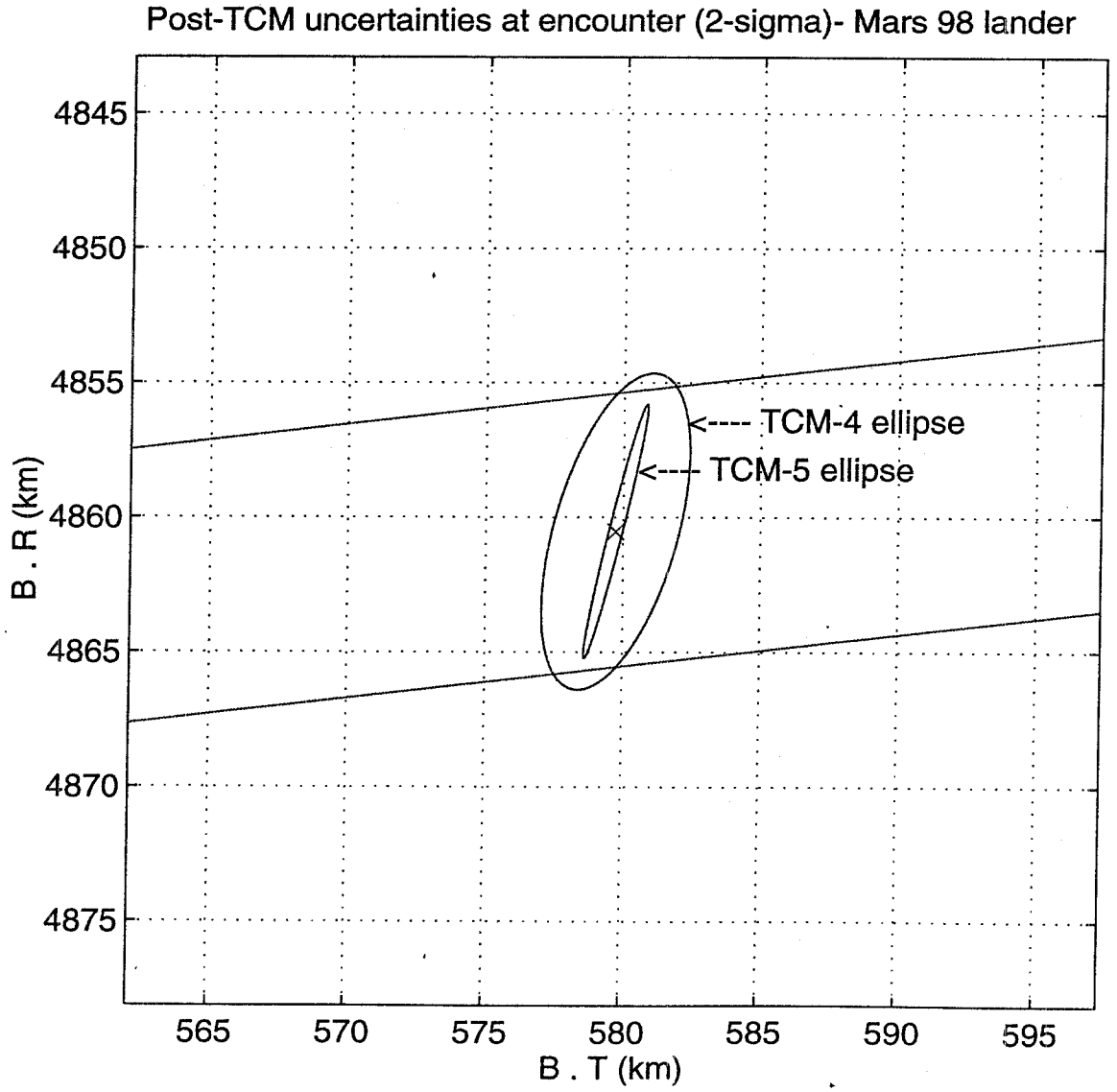

Maneuver ΔV Analysis

In addition to calculating the guidance errors, LAMBIC also determines the ΔV statistics (mean and sigma) of each midcourse maneuver. These data are used to determine the appropriate amount of propellant needed to complete the mission. To satisfy planetary quarantine requirements imposed by NASA, the launch vehicle injection coordinates must be designated such that there is less than one chance in 10,000 of the upper stage impacting Mars. This implies that the B-plane target for each launch vehicle may need to be biased from the ideal target. For the orbiter, this amounts to a B-plane bias of 109,660 km, while for the lander it is 41,230 km. Furthermore, this bias defines a non-zero 'deterministic' part of TCM-1, which is the size TCM-1 would be if there was no injection error (i.e. perfect injection). The deterministic part of TCM-1 is 20.9 m/s for the orbiter and 8.2 m/s for the lander. The remaining maneuvers have a deterministic part of zero. Since TCM-1 corrects for errors from injection, the ΔV statistics of TCM-1 are primarily a function of the launch vehicle's covariance and the deterministic part of TCM-1. The remaining maneuver sizes are primarily a function of the maneuver execution error model. Tables 5 and 6 give the mean, standard deviation and 95th-centile ΔV for all of the orbiter's and lander's maneuvers.

Monte Carlo Analyses

A high fidelity Monte Carlo simulation is used to determine lander descent propellant requirements, establish site elevation capability, and determine the range of entry timing parameters. This simulation, performed at Lockheed Martin Astronautics, uses 2000 approach states and entry masses derived from LAMBIC as inputs. The input data include guidance dispersions in the approach state due orbit determination errors, maneuver execution errors, and attitude control thruster mismodelling. Entry dispersions due to uncertainties and variability in the atmosphere are included using the statistical model in the MarsGRAM atmosphere program. A model of wind speed as a function of altitude is also included.

Table 5: Statistical results for orbiter ΔV

Maneuver	Mean	1σ	95%
TCM-1	30.94	13.65	56.67
TCM-2	1.37	1.04	3.48
TCM-3	0.45	0.55	1.57
TCM-4	0.12	0.18	0.47
Mission Total	32.89	13.65	57.33

Table 6: Statistical results for lander ΔV

Maneuver	Mean	1σ	95%
TCM-1	24.24	13.37	49.98
TCM-2	0.60	0.44	1.49
TCM-3	0.12	0.22	0.52
TCM-4	0.09	0.14	0.18
TCM-5	0.11	0.08	0.26
Mission Total	25.16	13.47	51.49

Entry aerodynamics, including variations in angle of attack, are modeled, as are errors in propagation of the onboard navigation state, and variability in the performance of the terminal descent propulsion system. Figure 11 shows the resultant landing footprint.

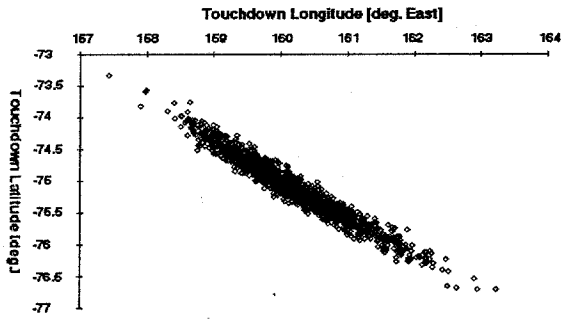

Figure 11: Landing footprint size determined from Monte Carlo analysis

The orbiter's orbit insertion propellant needs, ranges of capture orbit periods and on-orbit masses are also calculated using a Monte Carlo simulation program developed at JPL. Like the lander simulation, this program uses 2000 approach states as inputs, dispersed from the nominal primarily due to orbit determination and maneuver execution errors. Variations in propulsion I_{sp}, fuel mixtures, and orbit insertion pointing errors are modeled statistically, as are certain on-orbit maneuvers such as the transfer to map orbit.

Mars orbit insertion is modeled as a finite burn maneuver in this simulation. Other maneuvers, such as those associated with aerobraking, and attitude control fuel usage and contingency propellant are modeled as fixed ΔV or mass allocations.

Summary

Pre-flight analysis of interplanetary guidance errors for the Mars Surveyor '98 orbiter and lander have been performed for mission design. Both vehicles will rely on Doppler and range radio metric data collected at regular intervals, as well as careful modelling of the forces acting on the spacecraft. Following the orbiter's fourth midcourse maneuver at Arrival-10 days, the 3σ uncertainty in capture orbit periapsis radius is expected to be 35 km. This is larger than the ±20 km error requirement imposed by the project. However, it is anticipated that the error will be reduced with a more accurate error model for the momentum wheel desaturation maneuvers.

The lander has a tighter accuracy requirement, measured in the ability to achieve a flight path angle of -13.25°. This will be achieved by careful recording and modelling of the thruster activity controlling the vehicles attitude. Furthermore, by incorporating radio metric data from the orbiter during the final 30 days of the lander's cruise, a more accurate flight path estimate can be achieved. This technique of combining data from both spacecraft reduces orbit determination sensitivity to errors in tracking station locations, Earth orientation, Earth media delays and Mars ephemeris. The final lander flight path angle error is expected to be less than 0.27 degrees and 0.24 degrees upon completion of the fourth and fifth midcourse maneuvers, respectively.

Acknowledgments

The authors would like to acknowledge the contributions of Andre Sergeyevsky, Julie Kangas, Cliff Helfrich and David Spencer of JPL, and Bill Willcockson of Lockheed Martin Astronautics

The work described in this paper was performed at the Jet Propulsion Laboratory, California Institute of Technology, under contract with the National Aeronautics and Space Administration.

References

1. McNamee, Dr. John B., "The 1998 Mars Surveyor Lander and Orbiter Project." 35th Space Congress, Cocoa Beach, Florida, April 28 - May 1, 1998.

2. Mars Surveyor '98 Project Policies and Requirements Document (JPL internal document).

3. Vaughan, R. M., Kallemeyn, P. H., and Spencer, D. A., "Navigation Flight Operations for Mars Pathfinder System", Paper AAS-98-145, AAS/AIAA Astrodynamics Conference, Monterey, California, February, 1998.

4. Esposito, P., Alwar, V., Demcak, S., Graat, E., Johnston, M. and Mase, R., "Mars Global Surveyor Navigation and Aerobraking at Mars", Paper AAS 98-384, AAS/GSFC Int'l Symposium on Space Flight Dynamics, Greenbelt, Maryland, May, 1998.

5. Wang, T. C., Stanford, R. H., Sunseri, R. F., Breckheimer, P. J., "Survey of Optimization Techniques for Nonlinear Spacecraft Trajectory Searches," AIAA Paper No. 88-4285-CP, AIAA/AAS Astrodynamics Conference, Minneapolis, Minnesota, 1988.

6. Moyer, T. D., "Mathematical Formulation of the Double-Precision Orbit Determination Program (DPODP)", Technical Report 32-1527, Jet Propulsion Laboratory, Pasadena, CA, 15 May 1971.

7. Spier, G. W., "Design and Implementation of Models for the Double Precision Trajectory Program (DPTRAJ)", Technical Memorandum 33-451, Jet Propulsion Laboratory, Pasadena, CA, 15 April 1971.